*Clay Minerals*, (2007) **42**, 129–141

# Integration of Fe in natural and synthetic Al-pyrophyllites: an infrared spectroscopic study

S. LANTENOIS[1,2,*], J.-M. BENY[1], F. MULLER[1] AND R. CHAMPALLIER[1]

[1] *Institut des Sciences de la Terre d'Orléans (ISTO), CNRS – Université d'Orléans, 1A rue de la Férollerie, 45071 Orléans Cedex 2, France, and* [2] *Institut Charles Gerhardt (ICG-AIME), CNRS – Université Montpellier 2, Bât 15 – Case courrier 015, Place Eugène Bataillon, 34095 Montpellier Cedex 5, France*

(*Received 4 September 2006; revised 12 January 2007*)

ABSTRACT: Numerous studies focus on the relationships between chemical composition and OH-band positions in the infrared (IR) spectra of micaceous minerals. These studies are based on the coexistence, in dioctahedral micas or smectites, of several cationic pairs around the hydroxyl group which each produce a characteristic band in the IR spectrum. The aim of this work is to obtain the wavenumber values of the IR OH vibration bands of the (Al-$Fe^{3+}$)-OH and ($Fe^{3+}$-$Fe^{3+}$)-OH local cationic environments of 'pyrophyllite type' in order to prove, disprove or modify a model of dioctahedral phyllosilicate OH-stretching band decomposition. Natural samples are characterized by powder X-ray diffraction (XRD), Fourier transform infrared (FTIR) and Raman spectroscopies and electron microprobe; the hydrothermal synthesis products are also analysed by powder XRD and FTIR after inductively coupled plasma measurements to obtain the chemical compositions of starting gel phases. Natural samples contain some impurities which were eliminated after acid treatment; nevertheless, a small Fe content is found in the pyrophyllite structure. The amount of Fe which is incorporated within the pyrophyllite structure is much more important for the synthetic samples than for the natural ones. The IR OH bands were clearly observed in both natural and synthetic pyrophyllites and assigned to hydroxides bonded to (Al-Al), (Al-Fe) and (Fe-Fe) cationic pairs. During this study, three samples were analysed by DTG to check the *cis*- or *trans*-vacant character of the layers and to determine the influence of this structural character on the OH-stretching band position in IR spectroscopy.

KEYWORDS: pyrophyllite, hydrothermal syntheses, FTIR spectroscopy, Fe defaults, *cis*-*trans*-vacant.

Dioctahedral phyllosilicates have a wide spectrum of chemical composition (Bailey, 1988) and their cations distribute with different degrees of order-disorder in the tetrahedra and octahedra of the layer structure. Infrared spectroscopy is an efficient tool for the determination of local cationic environments as well as fine structural features. The main relationships between chemical composition and OH-band positions in the IR spectra of various dioctahedral materials have been established for celadonites and glauconites (Farmer, 1974; Velde, 1978; Slonimskaya *et al.*, 1986; Drits *et al.*, 1997), micas (Besson & Drits, 1997a,b; Velde, 1983) and smectites (Madejová *et al.*, 1994; Petit *et al.*, 2002; Fialips *et al.*, 2002a,b; Zviagina *et al.*, 2004; Gates, 2004). With advances in computer processing technology it has become possible to decompose the broad IR band of O–H vibrations of phyllosilicates.

Besson & Drits (1997a,b) established the relationships between the wavenumbers of the OH-

* E-mail: sebastien.lantenois@univ-montp2.fr
DOI: 10.1180/claymin.2007.042.1.09

stretching bands and the local cationic configuration around the hydroxyl group for dioctahedral *trans*-vacant micaceous minerals. This model was recently adapted to dioctahedral smectites by Zviagina *et al.* (2004). The model was based on the coexistence in dioctahedral micas or smectites of two important types of local cationic environment, 'mica-like' or 'pyrophyllite-like' depending on the presence or not of an interlayer cation. For the 'pyrophyllite-like' cationic environment, Besson & Drits (1997a,b) took into account three local cationic configuration possibilities around the hydroxyl group: (Al-Al), (Al-$Fe^{3+}$) and ($Fe^{3+}$-$Fe^{3+}$). The wavenumber value of the OH-stretching band of pyrophyllite (only one Al-Al cationic pair) $Si_4Al_2O_{10}(OH)_2$ is clearly identified (Farmer, 1974; Kloprogge & Frost, 1999; Wang *et al.*, 2002; Schroeder, 2002) in comparison with the wavenumber values of the other two cationic configurations (Al-$Fe^{3+}$)-OH and ($Fe^{3+}$-$Fe^{3+}$)-OH. The rare occurrence of natural ferripyrophyllite (Fe-rich equivalent of pyrophyllite described by Chukhrov *et al.*, (1978)) and the very small degree of Fe substitution in the natural pyrophyllite structure explain the lack of Fe-pyrophyllite IR studies.

The identification of the two (Al-$Fe^{3+}$)-OH and ($Fe^{3+}$-$Fe^{3+}$)-OH vibrations is necessary in order to prove, disprove or modify the model of dioctahedral phyllosilicate OH-stretching band decomposition. The aim of this study is to identify the IR OH-vibration bands in Fe-pyrophyllite structure. Two complementary approaches were carried out: the first consisting of the study of natural Fe-pyrophyllites and the second using hydrothermal synthetic samples. These samples have been characterized with FTIR coupled with chemical analyses, electron microprobe analyses (EMPA) and powder XRD.

## MATERIALS AND METHODS

### *Materials*

A variety of natural and synthetic samples was used in this study. The natural samples are described in Table 1. Synthetic pyrophyllites were crystallized from gels under hydrothermal conditions. Si-Al gels were prepared following the usual method adapted from Hamilton & Henderson (1968). Tetraethyl-orthosilicate (TEOS), $Al(NO_3)_3.9H_2O$, $HNO_3$, $NH_4OH$ and ethanol were used as reagents with a 99% minimum grade purity. After dissolution of Al-nitrate in nitric acid, TEOS and ethanol were added. A precipitate was obtained by neutralizing the resulting solution at pH ~6 with addition of $NH_4OH$. This precipitate was dried at 80ºC for 24 h, ground in an agate mortar and heated up to 400ºC to remove nitrates and to obtain a gel essentially composed of Si and Al oxides. Si-Al-Fe gels were prepared using sodium metasilicate ($SiO_2.Na_2O.5H_2O$), $AlCl_3.xH_2O$,$FeCl_3.6H_2O$ and HCl (Decarreau *et al.*, 1987) according to the reaction: $4(SiO_2.Na_2O) + x(AlCl_3) + (2-x)(FeCl_3) + 2HCl \rightarrow Si_4Al_xFe^{3+}_{2-x}O_{11} + 8NaCl + H_2O$.

Three $x$ values are used: 0.00, 0.40 and 1.75. After precipitation, the solid phase was washed and centrifuged to remove sodium chloride (five washings). Precipitates were dehydrated by drying

TABLE 1. Natural pyrophyllite samples examined.

| Name | Source | Minor phases associated* | Structure* |
|---|---|---|---|
| Rob 48 | Robbins, N. Carolina, BRGM collection | Mica traces | Monoclinic |
| Rob 49 | Robbins, N. Carolina, BRGM collection | Quartz and muscovite | Essentially monoclinic |
| Nep | Nepal**, Lantenois personal collection | – | Monoclinic |
| Van | Vanoise, France, ENS Paris collection, | – | Monoclinic |
| Sued | Sweden, Ref : 6534, Paris Museum collection | Muscovite and kaolinite | Monoclinic |
| SN | St. Niclaus valley, Zermatt, Swizerland. | – | Monoclinic |
| Bin | Besson personal collection*** | Quartz | Monoclinic |
| Guad | Guadeloupe (France), BRGM collection | Quartz | triclinic |

* determined by XRD
** more precise geographic locality not available
*** Besson & Drits (1997a,b)

at 60ºC over 24 h and ground in an agate mortar to obtain a gel composed essentially of Si, Al and Fe oxides (Grauby *et al.*, 1993). The samples were synthesized in an internally heated pressure vessel. 100 mg of gel were mixed with 100 mg of water in a gold tube. The tube was then sealed and heated under argon pressure. The experimental conditions and the chemical composition of the starting gel phases determined by inductively coupled plasma atomic emission spectroscopy (ICP-AES) are reported in Table 2. After cooling of the vessels, the solid products were extracted from the reaction tubes, dried at 80ºC overnight, and ground before structural and chemical characterization.

Some natural pyrophyllites containing additional phases were acid treated to remove these phases. Treated samples were prepared following an acid attack method adapted from Perez-Rodriguez *et al.* (1985) and Maqueda *et al.* (1986) known to destabilize all the phyllosilicate phases except pyrophyllite. A mixture of $HNO_3$, HF and $HClO_4$ was prepared. 100 mg of finely ground samples were placed in a Nalgène® reactor, mixed with 20 ml of deionized water, 2.5 ml of $HNO_3$ (68 wt.%), 2.5 ml of $HClO_4$ (60 wt.%) and 5 ml of HF (40 wt.%) and heated at 80ºC for 3 h. The residual solid part was filtered, washed with 100 ml of deionized water, dried by heating at 80ºC for 1 h and then ground before characterization.

## *Methods*

Natural and synthetic pyrophyllites were characterized by powder XRD. The patterns were recorded in transmission geometry using Co-*K*α radiation (35 mA, 35 kV). The use of an INEL® CPS 120 curved, position-sensitive detector allowed simultaneous recording of the diffracted intensity over a 4−50º2θ range with a step size of 0.03º. The non-linearity of the detector was corrected (Roux & Volfinger, 1996). A 0.5 mm diameter Lindemann glass tube was used to hold the sample powder.

The FTIR spectra of natural pyrophyllites were recorded over the 650−4000 $cm^{-1}$ range with a 2 $cm^{-1}$ resolution using a Nicolet® Magna 760 IR Fourier transform spectrometer equipped with a Globar® SiC source and a DTGS detector. The spectrometer was purged with dry air to remove most of the atmospheric $H_2O$ and $CO_2$ during data collection. Two recording methods were investigated. For natural samples the classical pellet preparation was used: the sample was finely ground in an agate mortar, and 0.5 mg of the resulting powder was mixed with 149.5 mg of KBr previously dried at 120ºC for 24 h. The mixture was homogenized and pressed in an evacuable die to prepare a 13 mm diameter pellet. For synthetic samples, IR spectra were recorded using the same Fourier transform spectrometer coupled with a Nicolet® Nic-Plan microscope to optimize IR signal and limit the amount of analysed sample. The powder was spread over the NaCl window of the microscope stage. The analysed sample area was a 100 μm diameter circle chosen under the microscope's 15× Cassegrainian objective. The operating conditions were 200 scans, 2 $cm^{-1}$ resolution over the 650−4000 $cm^{-1}$ range without ambient $H_2O$ correction.

The chemical compositions of the pyrophyllite samples were determined using a Cameca® SX50 electron microprobe (EMPA), operating at 15 kV accelerating voltage. The analysed samples were ground in an agate mortar and pressed in an

TABLE 2. Chemical and experimental data from synthetic pyrophyllites.

| Samples | PAl-1 | PAl-2 | PFe-1 | PFe-2 | PFe-3 |
|---|---|---|---|---|---|
| Chemical composition of starting gel phases* | | | | | |
| $SiO_2$ | 63.8 | 66.2 | 64.3 | 57.3 | 43.4 |
| $Al_2O_3$ | 36.2 | 33.8 | 28.9 | 5.0 | 0.0 |
| $Fe_2O_3$ | 0.0 | 0.0 | 6.6 | 36.6 | 56.4 |
| $Na_2O$ | 0.0 | 0.0 | 0.1 | 0.1 | 0.2 |
| Experimental conditions of hydrothermal synthesis | | | | | |
| Temperature (ºC) | 475 | 430 | 475 | 475 | 475 |
| Pressure (kbar) | 2 | 0.5 | 2 | 2 | 2 |
| Run time (days) | 15 | 29 | 15 | 15 | 15 |

* Oxide wt.% determined by ICP measurements

evacuable die in order to obtain a flat pellet necessary to achieve the best analytical results. A portion of each of the pellets was fixed on a glass slide and then silver metallized before analysis.

Raman spectra were obtained using a Dilor® XY 800 confocal micro Raman spectrometer equipped with a Wright Model charge-coupled detector (CCD). The excitation source was the 514 nm green line of a Coherent Innova Model 90-5 $Ar^+$ laser. The beam was focused onto powder samples placed on a glass slide using a 100× objective. Measurements were realized with a laser power of 100 mW and an integration time of 300 s.

The thermal gravimetric analyses (TGA) were recorded using a SETARAM® TGA 92 micro-analyser, with a heating rate of 10ºC/min. A 60 mg sample was used for each measurement. The derivative of the TG curve (DTG) gives the weight loss per ºC, which was assigned to water evolved from hydroxyl groups.

## RESULTS

### *Defaults in natural pyrophyllites*

The IR spectra (Fig. 1) in the OH-stretching zone (3600−3700 $cm^{-1}$) of some natural pyrophyllite samples (Table 1) indicate the presence of structural defaults. The (Al-Al)-OH stretching band of pyrophyllite is classically fixed near 3674 $cm^{-1}$ (Farmer, 1974; Fig. 1a). Associated with this intense vibration band, others at 3620, 3630, 3645, 3655, 3668 and 3698 $cm^{-1}$ were detected (Fig. 1b−e). Some of these vibration bands are associated with additional phyllosilicate phases. X-ray diffraction patterns (Fig. 2) also show the presence of associated mineral phases. Quartz was identified in the Rob49 (Fig. 2b) and Guad samples (Fig. 2c). Some other phyllosilicate minerals such as kaolinite were observed in the Sued sample (Fig. 2e) and muscovite in the Rob49 (Fig. 2b) and Sued samples (Fig. 2e). The associated phases detected by XRD are listed in Table 1.

These associated phases were eliminated with an acid treatment which allows kaolinite and mica phases to dissolve without destabilization of the pyrophyllite phase. Chemical analysis results using EMPA of the acid-treated pyrophyllite samples are given in Table 3. The disappearance of the OH-stretching bands corresponding to the associated phases is confirmed by FTIR analysis of the acid-treated samples (Fig. 3). The large band, characteristic of muscovite, near 3630 $cm^{-1}$ in sample Rob49 is missing (Figs 1b and 3b). In the Sued sample, the bands associated with kaolinite at 3620, 3655 and 3698 $cm^{-1}$ are not observed after acid treatment (Figs 1e and 3e). Nevertheless, some additional vibration bands were always present: e.g. a shoulder near 3668 $cm^{-1}$ in the Guad sample (Figs 1c and 3c) and a small band at 3645 $cm^{-1}$ in the SN and Sued samples (Figs 1d,e and 3d,e). Moreover, the vibration band at 3645 $cm^{-1}$ was also identified in three other samples presented in this study (Fig. 3f−h) and was correlated with the detection of Fe by EMPA (Table 3).

The OH-bending zone (800−1000 $cm^{-1}$) exhibits a band characteristic of pyrophyllite at 950 $cm^{-1}$ (Farmer, 1974) in all samples (Fig. 4a−h). Three other bands at 816, 836 and 855 $cm^{-1}$ were always present and generally observed in pyrophyllite

TABLE 3. Chemical formulae of pyrophyllites.

| Samples | Rob48 | Rob49 | Rob49-T | Sued | Sued-T | SN | SN-T | Bin | Guad | Nep | Van | PAl-1 | PAl-2 |
|---|---|---|---|---|---|---|---|---|---|---|---|---|---|
| Tetrahedral occupancy | | | | | | | | | | | | | |
| Si | 3.98 | 3.72 | 3.99 | 3.87 | 3.99 | 4.00 | 4.00 | 4.00 | 3.98 | 3.98 | 4.00 | 3.85 | 4.00 |
| Al | 0.02 | 0.28 | 0.01 | 0.13 | 0.01 | 0.00 | 0.00 | 0.00 | 0.02 | 0.02 | 0.00 | 0.15 | 0.00 |
| Octahedral occupancy | | | | | | | | | | | | | |
| Al | 2.00 | 1.96 | 1.99 | 2.20 | 1.97 | 1.97 | 1.97 | 1.97 | 2.00 | 1.98 | 1.97 | 2.00 | 1.98 |
| Fe | 0.00 | 0.00 | 0.00 | 0.03 | 0.03 | 0.03 | 0.03 | 0.03 | 0.00 | 0.02 | 0.03 | 0.00 | 0.00 |
| Interlayer cations | | | | | | | | | | | | | |
| K | 0.01 | 0.36 | 0.00 | 0.07 | 0.01 | 0.00 | 0.00 | 0.00 | 0.01 | 0.02 | 0.00 | 0.00 | 0.00 |
| Na | 0.01 | 0.04 | 0.00 | 0.01 | 0.00 | 0.00 | 0.00 | 0.00 | 0.00 | 0.01 | 0.00 | 0.00 | 0.00 |

All chemical formulae were calculated using electron microprobe analyses. −T after sample name indicates pyrophyllite samples after acid treatment.

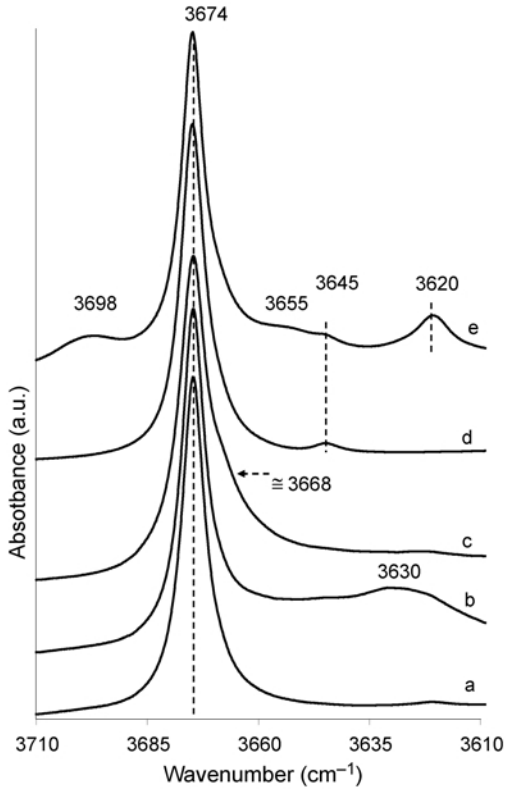


FIG. 1. IR spectra of natural pyrophyllites in the OH-stretching zone. (a) Rob 48, (b) Rob 49, (c) Guad, (d) SN, (e) Sued.

(Farmer, 1974). A very small band at ~907 cm$^{-1}$ could also be observed in some pyrophyllites samples (Fig. 4d–h) and was systematically correlated to the band at 3645 cm$^{-1}$ in the OH-stretching zone (Fig. 3d–h) and to the presence of Fe (Table 3). The link between these two bands and the presence of Fe in the structure is discussed below.

### *Integration of Fe in synthetic pyrophyllites*

An experimental run of hydrothermal syntheses was carried out in order to produce pyrophyllite with different Fe content. The experimental conditions are reported in Table 2 and in accordance with the stability domain of pyrophyllite identified by Eberl (1979) and established by Kloprogge & Frost (1999). X-ray diffraction patterns of synthetic samples are presented in Fig. 5. Only pyrophyllite reflections were identified (Fig. 5a) for the composition PAl-1. The second pyrophyllite (PAl-2) synthesized at different temperature/pressure conditions (Table 2) showed the same XRD pattern as sample PAl-1. After hydrothermal treatment, the two Al-Fe samples (PFe-1 and PFe-2) consisted of a mixture of hematite ($\alpha$-$Fe_2O_3$), opal ($SiO_2$, $xH_2O$) and pyrophyllite (Fig. 5c,d). The next synthetic compound, without Al (PFe-3), consisted only of hematite and opal (Fig. 5e).

The IR spectra of the synthetic pyrophyllite samples are presented in Fig. 6 (OH-stretching zone) and Fig. 7 (OH-bending zone). The presence of an OH-stretching vibration band at 3674 cm$^{-1}$ was observed in Al-pyrophyllite (PAl-1 and PAl-2) but was associated with another band at 3668 cm$^{-1}$ (Fig. 6a,b). The 3668 cm$^{-1}$ band was previously observed in the Guadeloupe natural pyrophyllite (Figs 1c and 3c). The intensity ratio between these two bands was different in samples PAl-1 and PAl-2. A possible assignment of these two bands is discussed below. In samples PFe-1 and PFe-2, these bands were still present, but two others were detected in addition, at 3645 cm$^{-1}$ as in natural Fe-containing pyrophyllite (Table 3, Fig. 3d–h) and at 3620 cm$^{-1}$ (Fig. 6c,d). In the OH-bending zone, a band near 950 cm$^{-1}$ was observed in all the synthetic samples (Fig. 7) as in the natural ones (Fig. 4). In samples PAl-1 and PAl-2, the three bands at 816, 836 and 855 cm$^{-1}$, characteristic of pyrophyllite (Farmer, 1974), are also present but two other bands were observed at 919 and 882 cm$^{-1}$ (Fig. 7a,b). In samples PFe-1 and PFe-2, two bands at 903 and 875 cm$^{-1}$ were detected and the presence of a Si–O vibration band of opal near 800 cm$^{-1}$ was also observed (Fig. 7c,d).

## DISCUSSION

### *The Al-Al-OH vibration bands*

*Identification of bands in the OH-stretching zone*. Generally, natural pyrophyllites are characterized by an IR absorption peak at ~3675 cm$^{-1}$ ((Al-Al)-OH vibration band; Farmer, 1974) and a dehydroxylation maximum temperature between 550 and 680ºC (Mackenzie, 1970; Schomburg, 1985; Sanchez-Soto & Perez-Rodriguez, 1989; Perez-Maqueda *et al.*, 2004).

The characteristic IR band was observed for all the natural and synthetic pyrophyllites presented in this study (Figs 1, 3 and 6). However, another

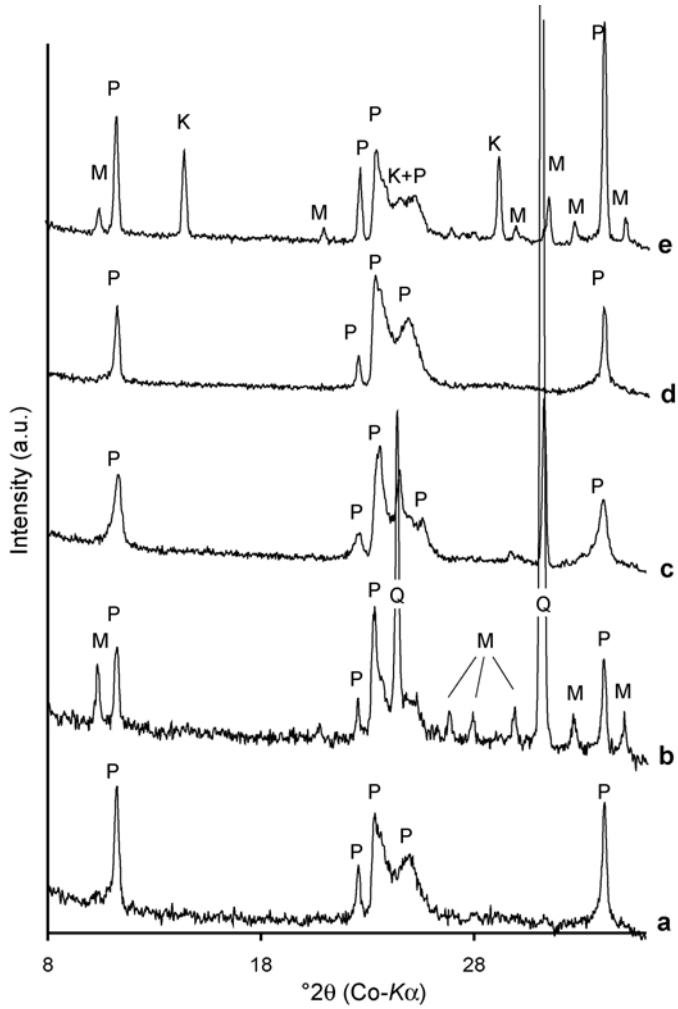


FIG. 2. XRD patterns of natural pyrophyllites: (a) Rob 48, (b) Rob 49, (c) Guad, (d) SN, (e) Sued. Pyrophyllite reflections are labelled P. Quartz, muscovite and kaolinite impurities are labelled Q, M and K, respectively.

hydroxyl environment was detected with a band close to 3668 $cm^{-1}$ identified as a shoulder in one natural sample (Guadeloupe sample, Fig. 3c) and as a peak in some synthetic samples (Fig. 6). Because the synthetic samples PAl-1 and PAl-2 contain only Al and Si (Table 2) and because only a pyrophyllite phase is detected in the powder XRD pattern (Fig. 5a,b), the band at 3668 $cm^{-1}$ can only be associated with an (Al-Al)-OH vibration of a pyrophyllite structure.

The presence of two hydroxyl aluminous structural environments was also observed in the thermal curves. The DTG curves of the three samples (Guad, PAl-1 and PAl-2), presented in Fig. 8 show two dehydroxylation peaks between 400 and 850ºC. The more intense peak was observed near 560ºC and the second peak near 780ºC. The existence of two different dehydroxylation temperatures is currently observed in some dioctahedral 2:1 phyllosilicates (Mackenzie, 1957; Grim, 1968; Drits *et al.*, 1995) and is correlated with the existence of *cis*- or *trans*-vacant layers (Drits *et al.*, 1995; Muller *et al.*, 2000b). Indeed, the layers of dioctahedral 2:1 phyllosilicates can differ in the distribution of the octahedral cations over the *cis*- and *trans*-vacant sites. In dioctahedral phyllosilicates, the octahedral sheet is composed of two cations and a vacancy around the OH group. If one

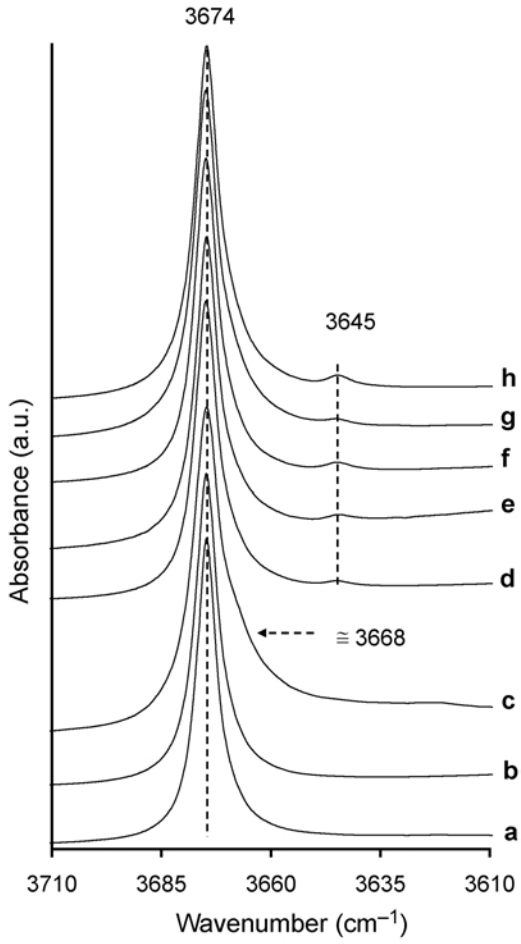


FIG. 3. IR spectra of pyrophyllites in the OH-stretching zone after acid treatment if necessary: (a) Rob 48-T, (b) Rob 49-T, (c) Guad-T, (d) SN-T, (e) Sued-T, (f) Bin, (g) Nep, (h) Van. For the three last samples, it was not necessary to perform acid treatment because phyllosilicate phases were not present as impurities in these samples.

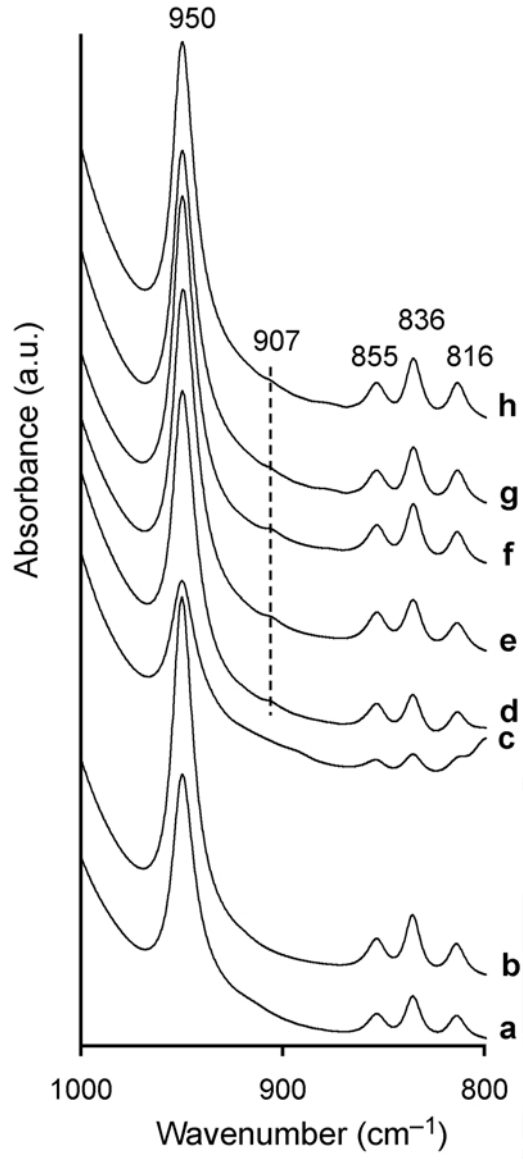


FIG. 4. IR spectra of pyrophyllites in the OH-bending zone after acid treatment if necessary: (a) Rob 48-T, (b) Rob 49-T, (c) Guad-T, (d) SN-T, (e) Sued-T, (f) Bin (g) Nep, (h) Van. For the three last samples, it was not necessary to perform acid treatment because phyllosilicate phases were not present as impurities in these samples.

cation is placed in a *trans* position and the second in one of the two *cis* 1 or *cis* 2 positions (*C*12(1) space group, Fig. 9a, Drits *et al.*, 1995), the structure is identified as a *cis*-vacant structure. On the contrary, if the two cations were placed in the two *cis* positions (*C*12/*m*(1) space group, Fig. 9b, Muller *et al.*, 200a,b) the structure is identified as a *trans*-vacant structure. Drits *et al.* (1995) assumed that thermal energy needed for a proton to jump to the nearest OH group to form a water molecule strongly depends on the distance between the nearest OH groups. Therefore a *cis*-vacant structure requires a greater dehydroxylation energy than a *trans*-vacant one because of the greater OH−OH distance (Muller *et al.*, 2000b). This is confirmed in

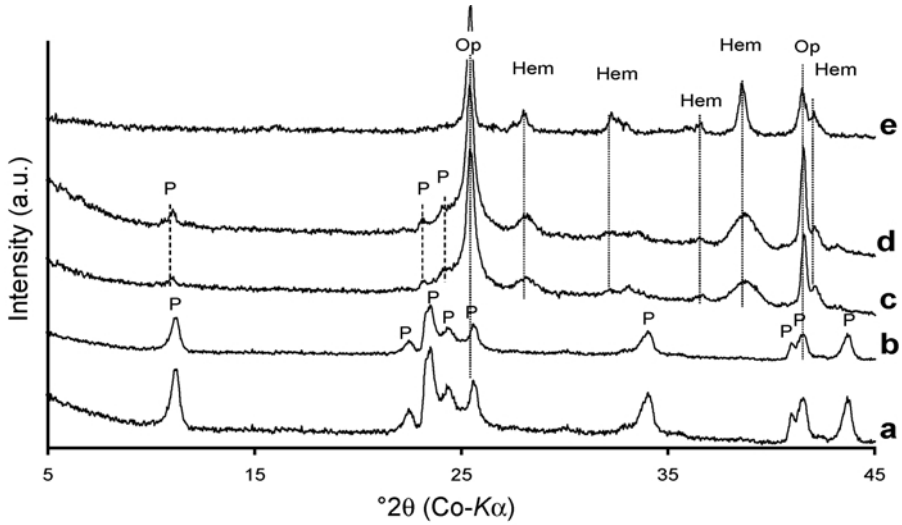


FIG. 5. XRD patterns of synthetic pyrophyllites: (a) PAl-1, (b) PAl-2, (c) PFe-1, (d) PFe-2, (e) PFe-3. Pyrophyllite reflections are labelled P. Associated opal and hematite phases are labelled Op and Hem, respectively.

the literature; *trans*-vacant dioctahedral phyllosilicates dehydroxylate between 550 and 680ºC and *cis*-vacant phyllosilicates dehydroxylate between 700 and 850ºC (Mackenzie, 1957, 1970, 1982; Heller-Kallai *et al.*, 1962; Trauth & Lucas, 1967; Grim, 1968; Brindley, 1976; Guggenheim, 1990; Tsipursky *et al.*, 1985; Drits *et al.*, 1995; Muller *et al.*, 2000a,b).

Although pyrophyllite minerals are classically identified as *trans*-vacant phyllosilicates (Wardle & Brindley, 1972; Muller *et al.*, 2000b) with a dehydroxylation maximum between 550 and 680ºC (Mackenzie, 1970; Schomburg 1985; Sanchez-Soto & Perez-Rodriguez, 1989; Perez-Maqueda *et al.*, 2004), Wang & Zang (1997a,b) identified three kinds of pyrophyllite populations. The first has a large DTG dehydroxylation peak with a maximum temperature near 650ºC and is identified as a *trans*-vacant structure. The second has a large DTG dehydroxylation peak with a maximum temperature near 880ºC and is identified as a *cis*-vacant structure. The third presents two maxima at 650 and 880ºC which correspond to a *cis*- and *trans*- mixture of pyrophyllite phases or an interstratification between *cis* and *trans* layers. For the three samples Guad, PAl-1 and PAl-2, the two structural OH losses near 550 and 750ºC could be interpreted as the presence of *trans*- and *cis*-vacant layers respectively. So, it can be considered that the presence of these two OH-stretching bands will be correlated with the existence of a structure partially *cis*- and partially *trans*-vacant. In this case, the band at 3674 $cm^{-1}$ will be characteristic of *trans*-vacant (Al-Al)-OH bands and the band at 3668 $cm^{-1}$ will be characteristic of *cis*-vacant (Al-Al)-OH.

*Correlation in the OH-bending zone*. In natural pyrophyllite (with *trans*-vacant structure; Muller *et al.*, 2000b; Wardle & Brindley, 1972), the (Al-Al)-OH band in the OH-bending zone is classically identified at ~950 $cm^{-1}$ (Russell *et al.*, 1970). This band was observed in all the pyrophyllite samples presented in this study (Figs 4 and 7).

For Al-synthetic samples (PAl-1 and PAl-2), two other bands were identified at 882 and 919 $cm^{-1}$ (Fig. 7a,b). The band near 880 $cm^{-1}$ is not included in the bending vibration range of (Al-Al)-OH (between 900 and 955 $cm^{-1}$) but is observed in a lot of synthetic dioctahedral 2:1 phyllosilicates (beidellite, pyrophyllite and montmorillonites: Kloprogge *et al*., 1990; Kloprogge & Frost, 1999; Lantenois *et al*., 2007). Because Russell *et al*. (1970) have observed this band in a synthetic deuterated pyrophyllite sample, it cannot be attributed without ambiguity to an OH-vibration band.

The band at ~919 $cm^{-1}$ is included in the (Al-Al)-OH bending range. Because the band at 950 $cm^{-1}$ is classically observed in *trans*-vacant pyrophyllites, we attribute the 919 $cm^{-1}$ band to the presence of *cis*-vacant layers of pyrophyllite. This

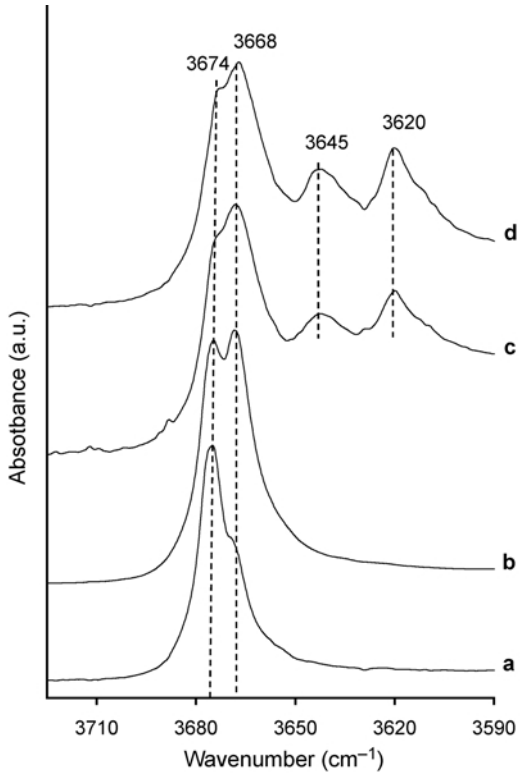


FIG. 6. IR spectra of synthetic samples containing a pyrophyllite phase in the OH-stretching zone: (a) PAl-1, (b) PAl-2, (c) PFe-1, (d) PFe-2.

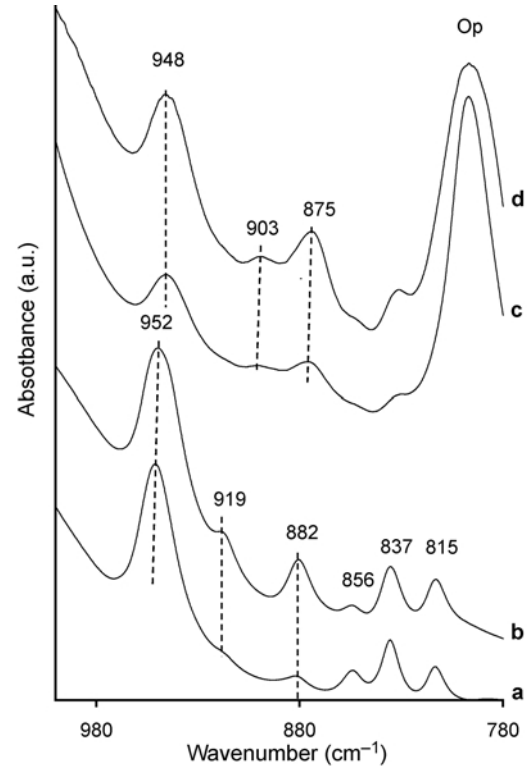


FIG. 7. IR spectra of synthetic pyrophyllites in the OH-bending zone. (a) PAl-1, (b) PAl-2, (c) PFe-1, (d) PFe-2.

interpretation is in accordance with the (Al-Al)-OH-bending band positions of different *cis*- and *trans*-vacant dioctahedral 2:1 phyllosilicates. Among dioctahedral smectites, most montmorillonites, consisting of *cis*-vacant 2:1 layers (Tsipursky & Drits, 1984) have the (Al-Al)-OH bending range between 910 and 920 $cm^{-1}$ (Madejová *et al.*, 2000; Madejová & Komadel, 2001; Gates, 2004; Lantenois *et al.*, 2005, 2007). For most beidellites, composed of *trans*-vacant layers, this range is 930–940 $cm^{-1}$ (Farmer, 1974; Gates, 2004; Kloprogge, 2006).

### *The OH-vibration bands linked to the incorporation of Fe*

*Identification of bands in the OH-stretching zone.* In all natural and synthetic Fe-containing samples (Table 3), a band at 3645 $cm^{-1}$ was observed (Fig. 3). Farmer & Russell (1964) proposed two possibilities for this band assignment: first it could

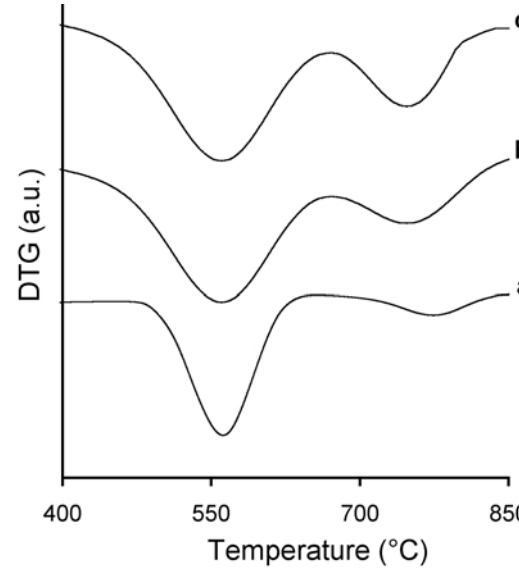


FIG. 8. DTG curves of pyrophyllites in the 400–850ºC temperature range: (a) Guad, (b) PAl-1, (c) PAl-2.

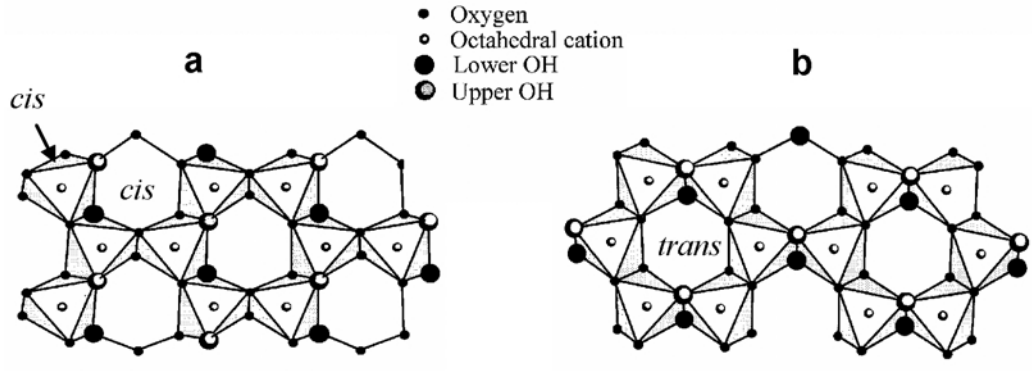


FIG. 9. A fragment of the octahedral sheet of a 2:1 layer showing the local disposition of the octahedral sites around the OH groups: (a) *cis*-vacant structure and (b) *trans*-vacant structure.

be interpreted as the symmetric OH vibration (the two hydroxyls groups vibrations are in phase) coupled to an antisymmetric vibration at 3675 $cm^{-1}$ (the two hydroxyl group vibrations are in phase opposition). In Raman and IR spectroscopy, the symmetric and antisymmetric bands generally have a reverse intensity ratio. The Raman spectrum of the VAN pyrophyllite sample (Fig. 10) shows that the symmetric and antisymmetric bands have the same wavenumber and are in the same intensity ratio as in the IR spectrum (Fig. 3g). This means that the first Farmer & Russell (1964) suggestion is incorrect. An alternative assignment proposed by Farmer & Russell (1964) and Besson & Drits (1997b) suggested that the band at 3645 $cm^{-1}$ could be attributed to an (Al-$Fe^{3+}$)-OH band. Moreover, Besson & Drits (1997b) developed a model which takes into account an (Al-$Fe^{3+}$)-OH band at 3652 $cm^{-1}$ and a ($Fe^{3+}$-$Fe^{3+}$)-OH band at 3630 $cm^{-1}$ correlated with an increase in the Fe content in the case of a 'pyrophyllite-like' cationic environment.

In synthetic samples PFe-1 and PFe-2, a band near 3620 $cm^{-1}$ was detected (Fig. 6c,d). In these samples only associated opal and hematite phases are detected by XRD (Fig. 5c,d). The only OH-bearing phase is an Fe-bearing pyrophyllite and the 3620 $cm^{-1}$ band is associated with an hydroxyl with an ($Fe^{3+}$-$Fe^{3+}$) environment. Moreover, in the hydrothermal conditions used, Fe previously introduced in ferric form cannot change during the synthesis (Decarreau *et al.*, 1987). Thus, in accordance with Farmer & Russell (1964) and Besson & Drits (1997b), if the 3645 $cm^{-1}$ vibration is assigned to the (Al-$Fe^{3+}$)-OH band, the 3620$cm^{-1}$ band must be associated with ($Fe^{3+}$-$Fe^{3+}$)-OH. This interpretation is confirmed by chemical analysis which, for synthetic samples, shows an increase in Fe content in comparison with natural ones (Tables 2 and 3).

*Comparison with the Fe analogue of pyrophyllite: ferripyrophyllite*. Ferripyrophyllite is the ferric analogue of pyrophyllite with an ideal formula $Fe_2^{3+}Si_4O_{10}(OH)_2$. This mineral is very rare and has only been described and characterized in its natural

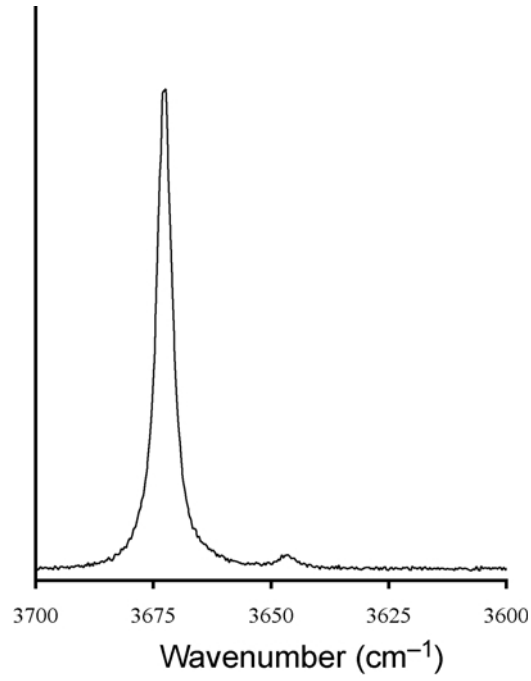


FIG. 10. Raman spectra of the VAN pyrophyllite sample in the OH-stretching zone.

state once, by Chukhrov e*t al.* (1978), and synthesized by Grauby (1993). We tried to synthesize ferripyrophyllite in the conditions fixed by Grauby (1993) and in the hydrothermal conditions used to synthesize our pyrophyllites: at 430ºC, 0.5 kbar, 29 days and at 475ºC, 2 kbar, 15 days. Ferripyrophyllite did not form in these conditions.

The IR study of the two natural minerals shows two bands in the OH-stretching zone. The first has a strong intensity and is fixed near 3590 $cm^{-1}$ and the second has a lower intensity and appeared near 3630 $cm^{-1}$ (Chukhrov e*t al.*, 1978). These two bands can be attributed to an ($Fe^{3+}$-$Fe^{3+}$)-OH band and to an (Al-$Fe^{3+}$)-OH band, respectively, in accordance with the chemical composition of this mineral established by Coey *et al*. (1984). In the synthetic sample, only the ($Fe^{3+}$-$Fe^{3+}$)-OH band was identified by Grauby (1993) near 3595 $cm^{-1}$. These data show shifts of 15 $cm^{-1}$ and 25 $cm^{-1}$, respectively, for the ($Al^{3+}$-$Fe^{3+}$)-OH and ($Fe^{3+}$-$Fe^{3+}$)-OH band positions between ferripyrophyllite (Chukhrov e*t al*., 1978; Grauby, 1993) and our synthetic samples.

These shifts can be explained by a difference in chemical composition. This phenomenon has already been observed in other phyllosilicates. For example, Wilkins & Ito (1967) observed shifts of <5 $cm^{-1}$ between the stretching-vibration bands of (Ni-Ni-Ni)-OH in the Mg-Ni talc series and proposed a correlation of the OH vibration band displacement with the ionic radius of the octahedral cations. These shifts were smaller than those obtained in this study, but the difference in ionic radii between Mg and Ni is very small (<0.03 Å, Shannon, 1976) in comparison with the difference between Al and ferric Fe ionic radii (0.11 Å, Shannon, 1976). Moreover, an important shift (near 20 $cm^{-1}$) depending on Fe content was observed by Gates (2004) in the IR spectra of dioctahedral smectites. For instance, the (Al-Fe)-OH bending band position shifted from 889 $cm^{-1}$ to 868 $cm^{-1}$ in accordance with an increase in Fe content in the octahedral sheet.

*Identification of bands in the OH-bending zone*. In natural pyrophyllite samples containing structural Fe, we observed systematically the presence of a band at 907 $cm^{-1}$ (Fig. 4). This band was identified as an ($Al^{3+}$-$Fe^{3+}$)-OH bending band and was shifted to 903 $cm^{-1}$ in synthetic pyrophyllite samples (Fig. 7c,d). An ($Fe^{3+}$-$Fe^{3+}$)-OH vibration band has been identified by Chukhrov *et al*. (1978) at 842 $cm^{-1}$ and between 800 and 805 $cm^{-1}$ by Grauby (1993). In this range, the presence of Si-O vibration bands and the three bands at 856, 837 and 815 $cm^{-1}$ currently observed in pyrophyllite and not assigned to OH-bending vibration (Russell *et al.*, 1970) hindered the detection of this vibration band. In addition, in our sample, a synthetic broad band associated with opal makes it impossible to identify this ($Fe^{3+}$-$Fe^{3+}$)-OH band (Fig. 7c,d).

## CONCLUSIONS

The integration of Fe in pyrophyllites has been studied. The spectroscopic data coupled with the chemical analyses of both natural and synthetic pyrophyllite samples have shown how it is possible that the pyrophyllite structure can incorporate ferric Fe. The presence of this structural Fe was associated with characteristic OH-vibration bands in the IR spectra. Vibration bands near 907 and 3645 $cm^{-1}$ were identified as (Al-Fe)-OH bending and stretching vibration bands respectively. An (Fe-Fe)-OH stretching band near 3620 $cm^{-1}$ was only identified in synthetic pyrophyllite samples, which were more Fe-rich than natural ones. The positions of these (Al-Fe)-OH and (Fe-Fe)-OH stretching bands confirmed experimentally the band positions suggested by Besson & Drits (1997a,b) in their model of decomposition of the OH-stretching bands for micaceous materials.

## ACKNOWLEDGMENTS

P. Baillif, O. Rouer (ISTO-Orléans), A. Pineau (CRMD-Orléans), L.-C. de Menorval (ICG-AIME Montpellier) and C. Reibel (ICG-PMDP Montpellier) are thanked for their assistance.

## REFERENCES

Bailey, S.W. (1988) *Hydrous Phyllosilicates*. Reviews in Mineralogy, **19,** Mineralogical Society of America, Washington, D.C., U.S.A.

Besson G. & Drits V.A. (1997a) Refined relationships between chemical composition of dioctahedral fine-grained micaceous minerals and their infrared spectra within the OH stretching region. Part I: identification of the OH stretching bands. *Clays and Clay Minerals*, **45**, 158−169.

Besson G. & Drits V.A. (1997b) Refined relationships between chemical composition of dioctahedral fine-grained micaceous minerals and their infrared spectra within the OH stretching region. Part II: The main factors affecting OH vibrations and quantitative analysis. *Clays and Clay Minerals*. **45**, 170−183.

Brindley G.W. (1976) Thermal transformations of clays and layer silicates Pp. 119–120 in: *Proceedings of the International Clay Conference 1975*, (J. Fripiat, editor), Applied Publishing Ltd., Wilmette, Illinois, USA.

Chukhrov F.V., Zvyagin B.B., Drits V.A., Gorshkov A.I., Ermilova L.P., Goilo E.A. & Rudnitskaya E.S. (1979) The ferric analogue of pyrophyllite and related phases. Pp. 55–64 in: *Proceedings of the International Clay Conference 1978*, Oxford.

Coey J.M.D., Chukhrov F.V. & Zvyagin B.B. (1984) Cation distribution, Mössbauer spectra, and magnetic properties of ferripyrophyllite. *Clays and Clay Minerals*. **32**, 198–204.

Decarreau A., Bonnin D., Badaut-Trauth D., Couty R. & Kaiser P. (1987) Synthesis and crystallogenesis of ferric smectite by evolution of Si-Fe coprecipitates in oxidizing conditions. *Clays and Clay Minerals*, **22**, 207–223.

Drits V.A., Besson G. & Muller F. (1995) An improved model for structural transformations of heat-treated aluminous dioctahedral 2:1 layer silicates. *Clays and Clay Minerals*, **43,** 718–731.

Drits V.A., Dainyak L.G., Muller F., Besson G. & Manceau A. (1997) Isomorphous cation distribution in celadonites, glauconites, and Fe-illites determined by infrared, Mössbauer and EXAFS spectroscopies. *Clay Minerals*, **32**, 153–179.

Eberl D.D. (1979) Synthesis of pyrophyllite polytypes and mixed layers. *American Mineralogist*, **64**, 1091–1096.

Farmer V.C. (1974) *The Infrared Spectra of Minerals* (V.C. Farmer, editor). Monograph **4**, Mineralogical Society, London.

Farmer V.C. & Russell J.D. (1964) The infrared spectra of layer silicates. *Spectrochimica Acta*, **20,** 1149–1173.

Fialips C.I., Huo D., Yan L., Wu J. & Stucki J.W. (2002a) Effect of Fe oxidation state on the IR spectra of Garfield nontronite. *American Mineralogist*, **87**, 630–641.

Fialips C.I., Huo D., Yan L., Wu J. & Stucki J.W. (2002b) Infrared study of reduced and reduced-reoxidized ferruginous smectite. *Clays and Clay Minerals*, **50**, 455–469.

Gates W.P. (2004) Infrared spectroscopy and the chemistry of dioctahedral smectites Pp. 125–168 in: *The Application of Vibrational Spectroscopy to Clay Minerals and Layered Double Hydroxides* (J.T. Kloprogge, editor). CMS Workshop Lectures, **13**, The Clay Minerals Society, Aurora, Colorado.

Grauby O. (1993) *Nature et étendue des solutions solides octaédriques argileuses. Approche par synthèse minérale*. PhD thesis, Poitiers University, France.

Grauby O., Petit S., Decarreau A. & Baronnet A. (1993) The beidellite-saponite series: an experimental approach. *European Journal of Mineralogy*, **5**, 623–635.

Grim R.E. (1968) *Clay Mineralogy*. International Series in the Earth and Planetary Sciences, McGraw-Hill Book Company, New York.

Guggenheim S. (1990) The dynamics of thermal decomposition in aluminous dioctahedral 2:1 layer silicates: a crystal chemical model. Pp. 99–107 in: *Proceedings of the 9th International Clay Conference*, **2**, (V.C. Farmer & Y. Tardy editors), Strasbourg, France.

Hamilton D.L. & Henderson C.M.B. (1968) The preparation of silicate compositions by a gelling method. *Mineralogical Magazine*, **36**, 832–838.

Heller-Kallai L., Farmer V.C., Mackenzie R.C., Mitchell B.D. & Taylor H.F.W. (1962) The dehydroxylation and rehydroxylation of triphormic dioctahedral clay minerals. *Clay Mineral Bulletin*, **5,** 56–72.

Kloprogge J.T. (2006) Spectroscopic studies of synthetic and natural beidellites: A review. *Applied Clay Science*, **31**, 165–179.

Kloprogge J.T. & Frost R.L. (1999) An infrared emission spectroscopic study of synthetic and natural pyrophyllite. *Neues Jahrbuch für Mineralogie, Monatshefte*, 62–74.

Kloprogge J.T., Jansen J.B.H. & Geus J.W. (1990) Characterization of synthetic Na-beidellite. *Clays and Clay Minerals*, **38**, 409–414.

Lantenois S., Lanson B., Muller F., Bauer A., Jullien M. & Plançon A. (2005) Experimental study of smectite interaction with metal Fe at low temperature: 1. Smectite destabilization. *Clays and Clay Minerals*, **53**, 597–612.

Lantenois S., Champallier R., Bény J.-M. & Muller F. (2007) Hydrothermal synthesis and characterization of dioctahedral smectites: a montmorillonite series. *Applied Clay Science* (submitted)

Mackenzie R.C. (1957) *The Differential Thermal Investigation of Clays*. Monograph **2**, Mineralogical Society, London.

Mackenzie R.C. (1970) *Differential Thermal Analysis.* Vol. I, Academic Press, London.

Mackenzie R.C. (1982) Down-to-earth thermal analysis. Pp 25–36 in: *Thermal Analysis* (B. Miller, editor). Wiley Heyden Ltd., Chichester, UK.

Madejová J. & Komadel P. (2001) Baseline studies of The Clay Minerals Society source clays: infrared methods. *Clays and Clay Minerals*, **49**, 410–432.

Madejová J., Komadel P. & Čičel B. (1994) Infrared study of octahedral site populations in smectites. *Clay Minerals*, **29**, 319–326.

Madejová J., Bujdak J., Petit S. & Komadel P. (2000) Effects of chemical composition and temperature of heating on the infrared spectra of Li-saturated dioctahedral smectites. (I) Mid-infrared region. *Clay Minerals*, **35**, 739–751.

Maqueda L.A., Perez-Rodriduez J.L. & Justo A. (1986)

Problems in the dissolution of silicates by acid mixtures. *Analyst*, **11**, 1107–1108.

Muller F., Drits V.A., Plançon A. & Besson G. (2000a) Dehydroxylation of $Fe^{3+}$, Mg-rich dioctahedral micas: (I) structural transformation. *Clay Minerals*, **35,** 491–504.

Muller F., Drits V.A., Plançon A. & Robert J.-L. (2000b) Structural transformation of 2:1 dioctahedral layer silicates during dehydroxylation-rehydroxylation reactions. *Clays and Clay Minerals*, **48**, 572–585.

Perez-Maqueda L.A., Montes O.M., Gonzalez-Macias E.M., Franco F., Poyato J. & Perez-Rodriguez J.L. (2004) Thermal transformation of sonicated pyrophyllite. *Applied Clay Science*, **24**, 201–207.

Perez-Rodriduez J.L., Maqueda L.A. & Justo A. (1985) Pyrophyllite determination in mineral mixture. *Clays and Clay Minerals*, **33**, 563–566.

Petit S., Caillaud J., Righi D., Madejová J., Elsass F. & Köster H.M. (2002) Characterization and crystal chemistry of an Fe-rich montmorillonite from Ölberg, Germany. *Clay Minerals*, **37**, 283–297.

Roux J. & Volfinger M. (1996) Mesures précises à l'aide d'un détecteur courbe. *Journal de Physique*, **IV**, 127–134.

Russell J.D., Farmer V.C. & Velde B. (1970) Replacement of OH by OD in layer silicates, and identification of the vibrations of these groups in infra-red spectra. *Mineralogical Magazine*, **37,** 869–879.

Sanchez-Soto P.J. & Perez-Rodriguez J.L. (1989) Thermal analysis of pyrophyllite transformations. *Thermochimica Acta*, **138**, 267–276.

Schomburg J. (1985) Thermal investigations of pyrophyllites. *Thermochimica Acta*, **93**, 521–524.

Schroeder, P.A. (2002) Infrared spectroscopy in clay science. Pp. 181–206 in: *Teaching Clay Science* (A. Rule & S. Guggenheim, editors). CMS Workshop Lectures, **11**, The Clay Minerals Society, Aurora, Colorado.

Shannon, R.D. (1976) Revised effective ionic radii and systematic studies of interatomic distances in halides and chalcogenides. *Acta Crystallographica A*, **32**, 751–767.

Slonimskaya M.V., Besson G., Dainyak L.G., Tchoubar C. & Drits V.A. (1986) The interpretation of the IR spectra of celadonites and glauconites in the region of the OH stretching frequencies. *Clay Minerals*, **21**, 377–388.

Trauth N. & Lucas J. (1967) Apport des méthodes thermiques dans l'étude des minéraux argileux. *Bulletin du Groupe Français des Argile*, **XIX-2,** 11–24.

Tsipursky S.I. & Drits V.A. (1984) The distribution of octahedral cations in the 2:1 layers of dioctahedral smectites studied by oblique texture electron diffraction. *Clay Minerals*, **19**, 177–192.

Tsipursky S.I., Kameneva M.Y. & Drits V.A. (1985) Structural transformation of $Fe^{3+}$-containing 2:1 dioctahedral phyllosilicates in the course of dehydration. Pp. 569–577 in: *Proceedings of the 5th Conference of the European Clay Groups* (J. Konta, editor), Prague.

Velde B. (1978) Infrared spectra of synthetic micas in the series muscovite – MgAl celadonite. *American Mineralogist*, **63**, 343–349.

Velde B. (1983) Infrared OH-stretch bands in potassic micas, talcs and saponites; influence of electronic configuration and site of charge compensation. *American Mineralogist*, **68**, 1169–1173.

Wang L. & Zhang Z. (1997a) Principles and methods of quantitative analysis on b-axis disorder in 2:1 dioctahedral phyllosilicate. *Chinese Science Bulletin*, **42**, 1908–1911.

Wang L. & Zhang Z. (1997b) Orientating structure of hydroxyls in 2:1 phyllosilicates. *Chinese Science Bulletin*, **42**, 321–324.

Wang L., Zhang M., Redfern S.A.T. & Zhang Z. (2002) Dehydroxylation and transformations of the 2:1 phyllosilicate pyrophyllite at elevated temperatures: an infrared spectroscopic study. *Clays and Clay Minerals*, **50**, 272–283.

Wardle R. & Brindley G.W. (1972) The crystal structures of pyrophyllite, 1Tc, and of its dehydroxylate. *American Mineralogist*, **57**, 732–750.

Wilkins R.W.T. & Ito J. (1967) Infrared spectra of some synthetic talcs. *American Mineralogist*, **52**, 1649–1661.

Zviagina B.B., McCarty D.K., Środoń J. & Drits V.A. (2004) Interpretation of infrared spectra of dioctahedral smectites in the region of OH-stretching vibrations. *Clays and Clay Minerals*, **52**, 399–410.